On the 'Atomic' Polarizabilities in Small Si(n) Clusters and the Dielectric Constant of Bulk Silicon

ARTICLE *in* THE JOURNAL OF PHYSICAL CHEMISTRY C · OCTOBER 2010

Impact Factor: 4.77 · DOI: 10.1021/jp1049765

2 AUTHORS:

Piet Th. van Duijnen
University of Groningen
110 PUBLICATIONS **3,479** CITATIONS
SEE PROFILE

Marcel Swart
Catalan Institution for Research and Advan…
155 PUBLICATIONS **3,434** CITATIONS
SEE PROFILE

On the 'Atomic' Polarizabilities in Small Si_n Clusters and the Dielectric Constant of Bulk Silicon†

Piet Th. van Duijnen*,‡ and Marcel Swart§

Theoretical Chemistry, Zernike Institute for Advanced Materials, University of Groningen, Nijenborgh 4, 9747 AG Groningen, The Netherlands, Institut de Química Computacional and Departament de Química, Universitat de Girona, Campus Montilivi, 17071 Girona, Spain, and Institució Catalana de Recerca i Estudis Avançats (ICREA), Pg. Lluís Companys 23, 08010 Barcelona, Spain

Received: May 31, 2010; Revised Manuscript Received: August 31, 2010

Applying the classical discrete reaction field (DRF) approach, which includes a treatment for the solution of the many-body polarization in complex systems, we calculated the mean atomic polarizability for a Si atom from the known molecular polarizability of Si_3. With only this parameter (6.16 Å^3, i.e., close to the free atom value), and the geometries as input, the *effective* atomic mean polarizabilities and their averages ($\langle\alpha\rangle_n = \langle\alpha\rangle(n)/n$) for the series Si_4-Si_{10} were calculated and found to be in excellent agreement with theoretical and experimental values. These $\langle\alpha\rangle_n$ are larger than the bulk value of 3.7 Å^3. We used the same input parameter for (by hand) constructed model systems up to $n = 4950$ with various geometries. For the larger clusters with the diamond lattice, we obtained the bulk value, implying that we "predicted" the dielectric constant of silicon almost from first principles. However, even the largest system is still too small for considering it as a real dielectric. In other lattices (primitive and face centered cubic), the $\langle\alpha\rangle_n$ are significantly smaller than 3.7 Å^3, which we attribute to the tighter packing in these lattices in comparison with that of the diamond structure. The behavior in all these systems can be easily understood by accounting properly for the local fields and for damping the interaction between induced dipoles. We show that there is no need for additional (e.g., "charge transfer") parameters.

I. Introduction

In the past decade, many experimental and theoretical papers addressed the determination of the atomic polarizability of Si in relatively small silicon clusters Si_n, with n ranging from 3 to about 30.[1−8] Authors expressed in general their surprise that these clusters are more polarizable than bulk silicon with its per atom polarizability of about 3.7 Å^3 (≈25 bohr^3) as obtained from the Clausius−Mossotti formula.[9] Moreover, the values obtained depend more or less strongly on the size and shape of the cluster under investigation. Authors have tried to correlate the differences to shape, interatomic distances, HOMO−LUMO gaps, etc. without convincing success. Usually, the method consists of measuring or calculating the system's *mean* polarizability ($\langle\alpha\rangle(n) = (\alpha_{xx} + \alpha_{yy} + \alpha_{zz})(n)/3$) by various techniques. The results are invariably expressed in the average polarizability per atom ($\langle\alpha\rangle_n = \langle\alpha\rangle(n)/n$).

We are surprised by the fact that nowhere in these papers is the local field mentioned (except in one case,[8] but clearly applied with inappropriate parameters). A new feature is the "site-specific" analysis of $\langle\alpha\rangle_n$ and its reconstruction, the parametrization being based on partitioning of local—or "on-site"—polarizations (under the influence of an external electric field) in contributions from a local isotropic polarizability *and* charge transfer (CT) in the nearby environment. [7,8] Even more surprising was a comment (or conclusion)[8] that "the difficulty to reproduce the polarizability of small clusters as well as the change of polarizability between consecutive clusters, which is governed by specific quantum mechanical effects that cannot be accounted for by [an] electrostatic scheme".

Recently, we addressed in several papers the problems associated with matching macroscopic properties and microscopic calculations, and how to solve them.[10−12] Here we want to emphasize the importance of a proper treatment of the local fields, in particular in small specimen, but also in the macroscopic sense. Our discrete reaction field (DRF)[13,14] approach in molecular calculations (QM/MM or completely classical) treats local fields explicitly, and therefore we intend to go somewhat further than the averages of computed values.

The organization of the present paper is as follows. In the next section, we will address some formal issues like polarizability/size/shape relations, how discrete polarizabilities "interact", and how the classical many-body polarization problem can be solved. Next, we report results of completely classical calculations on Si_n clusters, $n = 3-10$, whose molecular polarizabilities are known, and compare them with the work of others. The same exercise is repeated and extended for model systems with $n = 5-4950$ with various crystal-like structures, in an effort to catch the essence of dielectric behavior.

Finally, we give a summary and conclusions.

II. Matching Macro- and Microscopic Descriptions of Matter

A. Microscopic View. The polarizability $\vec{\vec{\alpha}}$ of a system is defined as the parameter describing the (linear) response in an external electric field $\vec{F}$ as

$$\vec{\mu}_{ind} = \vec{\vec{\alpha}}\vec{F} \tag{1}$$

with $\vec{\mu}_{ind}$ the induced dipole moment. We note that $\vec{\vec{\alpha}}$ in general is anisotropic, the anisotropy usually defined as

† Part of the "Mark A. Ratner Festschrift".
‡ University of Groningen.
§ Universitat de Girona and ICREA.

10.1021/jp1049765
Published on Web 10/20/2010

$$\varsigma = \frac{\alpha_{max} - \alpha_{min}}{\langle\alpha\rangle} \tag{2}$$

where α_{max} and α_{min} are, respectively, the largest and smallest eigenvalue of $\vec{\vec{\alpha}}$ and $\langle\alpha\rangle = (\alpha_{xx} + \alpha_{yy} + \alpha_{zz})/3$ is the mean value.

We stressed already earlier[10] that a system has only a single observable polarizability or susceptibility. The reconstruction, or analysis, based on local contributions is in fact an abstraction, the result of which depends on the detail wanted, e.g., from atomic and/or bond or group polarizabilities. Atomic polarizable atoms and other localized contributions in molecules and solids are—like atomic charges and radii—*not* observable: they depend on the partitioning and interaction models, no matter how precise the latter are defined. They are important for analytical use or as parameters, e.g., in force fields[13] in which they are indispensable. However, they are only meaningful within the same partitioning and interaction schemes by which they are defined.

With this in mind, we look at n polarizable objects placed in an electric field. The induced dipole on site p is then given by

$$\vec{\mu}_p = \vec{\vec{\alpha}}_p[\vec{F} + \sum_{q\neq p}\vec{\mu}_q\vec{\vec{t}}_{pq}] \tag{3}$$

with $\vec{\vec{t}}_{pq}$ the electric field at p from a unit dipole in q. These contributions define the "local field", i.e., the difference between the applied field $\vec{F}$ and the actual field at p.

From eq 3 we get a self-consistent solution for all induced dipoles:

$$\vec{M} = \vec{\vec{\alpha}}[\vec{F} + \vec{\vec{T}}\vec{M}] \qquad \text{or} \qquad \vec{M} = \vec{\vec{A}}\vec{F} \tag{4}$$

with $\vec{\vec{\alpha}}$ the (block-diagonal) matrix formed by $\vec{\vec{\alpha}}_p$ and $\vec{\vec{T}}$ the collection of $\vec{\vec{t}}_{pq}$'s. The $3n \times 3n$ matrix

$$\vec{\vec{A}} = [\vec{\vec{\alpha}}^{-1} - \vec{\vec{T}}]^{-1} \tag{5}$$

is a "normal" polarizability in the sense that $\vec{M} = \vec{\vec{A}}\vec{F}$, i.e., a many-particle extension of eq 1. Note that $\vec{\vec{T}}$ contains only geometrical parameters: the distances and relative orientations of the various parts of the system. This makes immediately clear that the resulting many-body polarizability depends on the size and shape of the system. In ref 10 some examples for model systems may be found.

The dimension of $\vec{\vec{A}}$ can be reduced by summing the blocks of the various partitions:

$$\vec{\vec{\alpha}}^{G} = \sum_{i,j}^{N_G}(A_{ij})_{mn} \qquad m, n \in \{x, y, z\} \tag{6}$$

which for $N_G = n$ yields the system's total polarizability tensor. The matrix $\vec{\vec{\alpha}}^{G}$ is the effective polarizability of group (molecule or atom) G in its environment. From that we get mean isotropic effective polarizabilities $\langle\alpha^{eff}\rangle^{G}$ in the usual way. These mean effective polarizabilities are obviously not transferable because the influence of G's environment is included. In contrast, the atomic polarizabilities that are needed as input can be transferable.

For $n > 2$ solutions of eq 5 can only obtained by numerical techniques, but for $n = 2$ it can be solved exactly, then leading to Silberstein's equations:[15]

$$\alpha_{\parallel} = \frac{\alpha_1 + \alpha_2 + 4\alpha_1\alpha_2/r_{12}^3}{1 - 4\alpha_1\alpha_2/r_{12}^6}$$

$$\alpha_{\perp} = \frac{\alpha_1 + \alpha_2 - 2\alpha_1\alpha_2/r_{12}^3}{1 - \alpha_1\alpha_2/r_{12}^6} \qquad (r_{12}^6 > 4\alpha_1\alpha_2) \tag{7}$$

From eq 7 we learn that the total "molecular" polarizability is anisotropic, even if it is constructed from two isotropic polarizabilities. We see that $\alpha_{\parallel}$ will be larger than $(\alpha_1 + \alpha_2)$, due to the head-to-tail coupling of the induced dipoles along the axis. The dipoles perpendicular to the axis, which contribute to $\alpha_{\perp}$, obviously lower the total dipoles induced on the atoms.

For a distance $r_{12} \leq (4\alpha_1\alpha_2)^{1/6}$ a "polarization catastrophe" emerges with $\alpha_{\parallel}$ infinite or negative. This can be avoided by damping the interaction between the induced dipoles, e.g., with Thole's scheme,[16] in which a reduced interaction distance $u_{12} = r_{12}/(\alpha_1\alpha_2)^{1/6}$ is used, for which the interaction tensor is defined by

$$T_{12,ij} = (\alpha_1\alpha_2)^{1/2}\frac{\partial^2\phi(u_{12})}{\partial u_{12,i}\partial u_{12,j}} \qquad i, j \in \{x, y, z\} \tag{8}$$

with $\phi(u)$ the potential of a point charge at u. By assuming the polarizability is associated with a model charge distribution $\rho(u)$, we get

$$T_{12,ij} = \frac{3f_T r_i r_j}{r^5} - \frac{f_E r}{r^3} \qquad i, j \in \{x, y, z\} \tag{9}$$

in which the damping factors f_T and f_E depend on the form of $\rho(u)$.

We use exclusively the exponentially decaying distribution

$$\rho(u) = \frac{a^3}{8\pi}\exp(-au) \qquad a = \text{screening length} \tag{10}$$

from which the following factors are obtained for, respectively, the potential, field, and field gradient:

$$\begin{aligned} &v = au \\ &V = f_V/r \qquad f_V = 1 - \left(\frac{1}{2}v + 1\right)e^{-v} \\ &E_i = f_E r_i/r^3 \qquad f_E = f_V - \left(\frac{1}{2}v^2 + \frac{1}{2}v\right)e^{-v} \\ &T_{ij} = \frac{3r_i r_j f_T - \delta_{ij}r^2 f_E}{r^5};\ f_T = f_E - \frac{1}{6}v^3 e^{-v} \end{aligned} \tag{11}$$

i.e., factors going smoothly to unit for large r.

Equation 7 can also be used for *decomposing* the total (molecular) polarizability into *effective* atomic polarizabilities, e.g., for $\alpha_1 = \alpha_2$,

$$\alpha_1^{eff} = \alpha_2^{eff} = \frac{\alpha_{\parallel} + 2\alpha_{\perp}}{6} \tag{12}$$

or, in general, by assigning the $\vec{\vec{A}}_{PQ}$ and $\vec{\vec{A}}_{QP}$ in eq 6, respectively, to groups P and Q, and averaging the diagonal terms in the

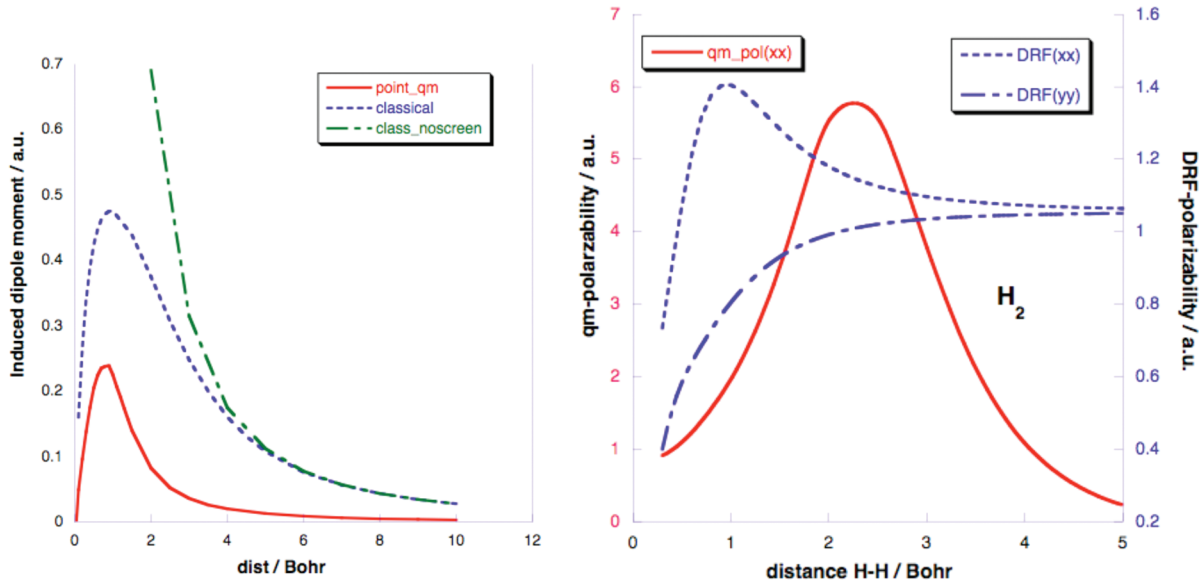

Figure 1. Effects of Thole's damping in simple systems. Left: dipole moment of H_2^+ (DRF/QM/MM). Right: polarizability of H_2 (QM and DRF).

resulting matrices. Other partitioning schemes are feasible but do not pay off the additional computing effort.[17]

The heart of our mixed quantum chemical/classical (QM/MM) and classical (MM) DRF approach is eq 5 (with Thole's interaction model). By fitting the set $\{\alpha_p\}$ to experimental or computed molecular polarizabilities, we generate a set $\{\alpha_T\}$ of transferable (model) polarizabilities for the constituting atoms from which other molecular polarizabilities can be computed within experimental accuracy.[16,18,19] For an extensive review see ref 10 and references given there.

Figure 1 depicts the effect of damping on a hydrogen atom, from quantum chemical calculations (i.e., a DRF/QM/MM model of H_2^+) and classical DRF (MM) calculations. It shows that Thole's scheme catches the essential events on going from large to very small interatomic distances. The differences between the QM, QM/MM, and MM results are associated with the difference between the polarizabilities as obtained from QM and DRF calculations: the $\{\alpha(\mathrm{DRF})\}$ come from fitting to experimental molecular polarizabilities, which cannot be easily matched by simple QM calculations.[19]

B. From Macroscopic to Microscopic, and Back. Starting from the macroscopic end, a dielectric is defined as a homogeneous and isotropic continuum with the dielectric constant, ε (≥ 1), as its only response parameter. The interaction between charges in the medium is then given by

$$U_{ij} = \frac{Q_i Q_j}{\varepsilon R_{ij}} \tag{12a}$$

with the Q's charges and R_{ij} their distance. Here ε acts as a *uniformly reducing* factor, uniform in the sense that it reduces the interaction between charges independent of their type (plus or minus). The charges should be at macroscopic distances and at macroscopic distances from any boundary of the system.

The embedded charges are supposed to be situated in (spherical) cavities, the size of which is microscopic with respect to the dimensions of the system. The charges polarize the continuum, the effects of which are usually represented by charges on the surfaces defining the cavities. The interaction energy between the Q's of eq 12 can then be formulated as

$$\begin{aligned} U_{ij} &= U_{ij}^{\mathrm{vac}} + U_i^{\mathrm{self}} + U_j^{\mathrm{self}} + U_{ij}^{\mathrm{int}} \\ &= \frac{Q_i Q_j}{R_{ij}} + (Q_i V_i^{S_i} + Q_j V_j^{S_j}) + (Q_i V_j^{S_i} + Q_j V_i^{S_j}) \end{aligned} \tag{13}$$

Here $V_i^{S_j}$ is the potential of the charges on the surface of i induced by Q_i and $V_j^{S_i}$ is the contribution due to Q_j. The induced surface charge of a single charge Q is obtained from the Born equation:[20]

$$Q^* = -\left(1 - \frac{1}{\varepsilon}\right)Q \tag{14}$$

independent of the size of the cavity. Other contributions depend on the positions of other charges. For large R_{ij} the screened interaction terms in eq 13 may vanish and for this case it can be shown that

$$U_{ij} \approx U_{ij}^{\mathrm{vac}} + \frac{1}{2}(Q_i^* Q_j + Q_j^* Q_i)/R_{ij} \tag{15}$$

Inserting the Q^* of eq 14 into eq 15, leads to eq 12a. In other words, a system behaves as a dielectric if charges are so far apart that only the self-interaction contributes to the induction energy.

The discussion above shows formally why the distances between sources of fields in a dielelectric should be macroscopic, but not why these sources should be also macroscopically far from boundaries.

In older work from our group[21] we reported efforts to build a dielectric from the microscopic world by putting two charges in a collection of polarizabilities. By varying the number of polarizabilities around and between the charges, we investigated the various contributions to the interaction energy. Of course, one gets eq 13 back in a slightly different form:

$$\begin{aligned} U_{ij} &= U_{ij}^{\mathrm{vac}} + U_i^{\mathrm{self}} + U_j^{\mathrm{self}} + U_{ij}^{\mathrm{int}} \\ &= \frac{Q_i Q_j}{R_{ij}} + (Q_i \sum_i V_i^{\mu_i} + Q_j \sum_j V_j^{\mu_j}) + (Q_i \sum_j V_j^{\mu_i} + Q_j \sum_i V_i^{\mu_j}) \end{aligned} \tag{16}$$

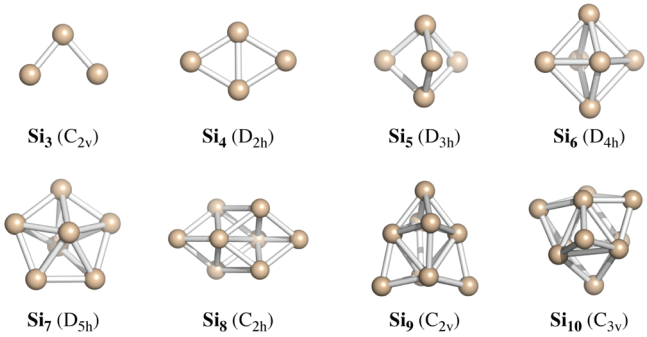

Figure 2. Si clusters studied here according to Pouchan.[4]

where $V_i^{\mu_j}$ is the potential of the dipole induced by Q_i in point j.

In small systems, i.e., with a small number of embedding polarizabilities and short distances between the charges, unlike charges attract each other more than in vacuum ("ε" < 1!), while like charges—if close enough—start to attract each other ("ε" < 0!). The common trend is that charges tend to move toward the "interaction" dipoles. When the number of slabs of polarizabilities between the charges is increased until the energy is completely determined by the self-interactions, at least all interactions are smaller than in vacuum. So far, we were in the same situation as above with the continuum model. However, the reduction of interaction between unlike and like charges was still different. This is caused by the local asymmetry: the charges are still too close to the boundaries of the finite system so that there are more induced dipoles "inside" than "outside" the charges' positions. To reach the "truly" dielectric behavior—uniform scaling, it was necessary to embed the complete discrete system in a continuum.

Jackson[22] states, as a rule of thumb for the minimum amount of matter before it can be treated as a dielectric, it must have a volume larger than $10^2 \times 10^2 \times 10^2$ Å^3. None of the Si clusters studied so far are large enough to consider them macroscopic.

III. Computational Details

All calculations reported here were classical (cf. eq 5) using DRF90[13,14] for computing (molecular) polarizabilities. We used throughout Thole's exponential damping[16,18,19] scheme.

IV. Results and Discussion

A. Systems Si_3−Si_{10}. First, we determined the necessary transferable atom polarizability for a Si atom. We took Si_3 in the C_{2v} geometry of Pouchan et al.[4] who computed a polarizability of 16.02 Å^3. With that and Pouchan's coordinates as input in eq 5, and taking $a = 2.1304$ (the default value in DRF90[13]), we found $\alpha_{Si} = 6.16$ Å^3, which is very close to the free atom values of 6.8 and 5.9 Å^3, respectively found from numerical calculations[23] and reported by Jackson et al.[2] The difference between α_{Si} and the free atom value is to be expected,[14,16,18] because the former is related to bound atoms.

Next, we computed the $\langle\alpha\rangle_n$ of the Si_n with $n = 4 - 10$ (see Figure 2), again using Pouchan's coordinates. The results are in Table 1.

In Table 1 we see that the DRF results are in perfect agreement with Pouchan's data, while using only a single training molecule for obtaining a single α_{Si}. Moreover, there is no need to take more parameters than the single transferable α_{Si}. Jackson et al.[7] divided their integration grid into "atomic" and "interstitial" regions. Dipoles induced by a weak electric field in the "atomic" regions were used for defining the "atomic" polarizabilities, while dipoles originating from the charge shifts in the interstitial volumes lead to charge transfer (CT) polarizabilities.

TABLE 1: Calculated and Experimental Averaged Mean Atomic Polarizabilities

	$\langle\alpha(n)\rangle/n$Å^3			
Si_n	B3LYP[a]	DRF[b]	lit.[a]	$\Delta_{DRF\text{-}B3LYP}$[d]
Si_3[c]	5.37	5.37	5.24 (0.02)	0.00
Si_4	5.14	5.18	5.08 (0.01	0.01
Si_5	4.99	4.90	4.87 (0.06)	0.02
Si_6	4.58	4.74	4.30 (0.24)	0.03
Si_7	4.49	4.61	4.45 (0.08)	0.03
Si_8	4.69	4.64	4.58 (0.08)	0.01
Si_9	4.53	4.64	4.38 (0.00)	0.02
Si_{10}	4.49	4.34	4.28 (0.04)	0.03[d]

[a] From ref 4. In parentheses, standard deviation in reported values. [b] This work. Coordinates from ref 4. [c] Training molecule for obtaining $\alpha_{Si} = 6.16$ Å^3. [d] $\Delta = |\alpha_{DRF} - \alpha_{B3LYP}|/\alpha_{B3LYP}$.

However, this rather cumbersome procedure—there only used for analytical purposes for Si_3 and Si_{26}—is based on just another partitioning scheme for splitting up expectation values of electronic properties. Although probably useful, they are all arbitrary because electrons do not want to be localized.

Guillaume et al.[8] tried a parametrization like in eq 5, using atomic polarizabilities, but extended with CT parameters based on induced Mulliken charges[24,25] (just another arbitrary choice!). Instead of fitting, they tried various values for α_{Si}, starting with the bulk value of 3.7 Å^3. That was unfortunate, because this value stems from the Clausius−Mossotti equation:

$$\alpha = \frac{3}{4\pi}\frac{\varepsilon - 1}{\varepsilon + 2}\Omega \tag{17}$$

with Ω the bulk atomic volume. In this equation the local fields are accounted for[26] and hence give the *effective* polarizability, which should not be used with a different internal field. At first they obtained too large values for $\langle\alpha\rangle_n$ because they clearly did not apply any damping in the (induced) dipole/dipole interaction. Hence, they tried smaller values to come closer to the calculated $\langle\alpha\rangle_n$ in their systems and tried to repair their best results by mixing in CT contributions.

We repeated their undamped "polarization only" exercises for the present systems and obtained similar values, as displayed in Figure 3.

First, we see that the two choices for α_{Si} (25 and 20 au) do not work: they give either too large or too small values for $\langle\alpha\rangle_n$ and lead to erratic results. The undamped example with the larger α_{Si} failed in our case for $N > 7$ because of the "polarization catastrophe": the inversion of $\overleftrightarrow{A}$ in eq 5 was not possible. The occurrence of this problem obviously depends on the use of specific software and on machine accuracy. It is demonstrated in Figure 4 for Si_2: the damped polarizability remains positive, while the undamped value first goes up too fast and then abruptly goes to −7 Å^3.

Note that our (damped) results in Figure 3 follow Pouchan's B3LYP results much closer than any of the efforts of Guillaume et al.,[8] with CT corrections or not.

Atomic polarizabilities in our DRF model were introduced to "construct" molecular polarizabilities for cases where QM calculations are impossible or impractical and to describe the small charge shifts occurring in weak external or intermolecular electric fields. They do just that.

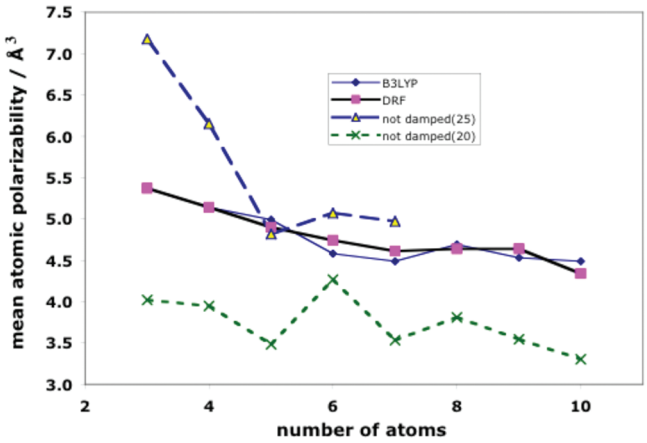

Figure 3. Mean atomic polarizabilities in S_n ($n = 3, 10$) with Pouchan's geometries.[27] B3LYP: from ref 4. DRF: this work (cf. Table 1) with damping (cf. eqs 9−11). Not damped: $\alpha_{Si} = 20$ and 25 au (3.0 and 3.7 Å^3).

Our dipole conserving population analysis of electronic charge distributions[28,29] is based on the reconstructing of induced dipoles on atoms in a molecule, by putting additional charges on other atoms nearby. This can obviously also be applied for "classical" systems, e.g., for two hydrogen bonded water molecules, which results in the same "charge transfer" as in the fully quantum chemical supermolecular treatment.[30] Here we applied this scheme on Si_5 under the influence of fields of strength 0.001 au in the *X*, *Y*, and *Z* directions and obtained the atomic dipoles and corresponding induced charges of Table 2.

The induced charges are typically of the same order as those reported by Jackson et al.[7] (Guillaume et al.[8] do not give specific numbers, but they try to improve their "polarization only" with fields of induced Mulliken charges. In passing we note that the latter are not all that good for predicting dipoles![28]). It will be clear that in the DRF approach there is no need for additional parameters. Our analysis shows that most "charge transfer" in the weak fields mentioned above is just polarization and should be treated as such. We are convinced that a single transferable

TABLE 2: Induced Dipoles and Corresponding Induced Charges of Si_5 in Fields of 0.001 au

		dipole moment/au			charges/e		
atom	field	*X*	*Y*	*Z*	*X*	*Y*	*Z*
1	*x*	0.024	0.0	0.000	0.000	0.000	0.34
	y	0.000	0.027	0.000			
	z	0.0	0.0	0.049			
2	*x*	0.027	0.0	0.0	0.000	−0.030	0.000
	y	0.000	0.042	0.000			
	z	0	0.0	0.027			
3	*x*	0.027	0.0	0.0	0.000	−0.030	0.000
	y	0.000	0.042	0.000			
	z		0.0	0.027			
4	*x*	0.042	0.0	−0.011	0.029	0.000	0.017
	y	0.000	0.026	0.000			
	z	−0.011	0.0	0.030			
5	*x*	0.042	0.0	0.011	−0.029	0.000	−0.017
	y	0.000	0.026	0.000			
	z	0.011	0.0	0.030			

"atomic" polarizability with a "global" screening distance is sufficient to pass easily from quantum chemical to classical descriptions and their combination.

Unfortunately, only Pouchan[27] gives useful structural information: in other publications one finds only pictures of "optimized" structures. Some structural information is also available in ref 31, but no polarizabilities are given there. Calculation of the polarizabilities of systems given there is not within the scope of this paper, but we intend to try that later.

The fixation of most authors on the *average* of atomic polarizabilities leads to destruction of information. From our calculations, we obtain the actual effective polarizability matrices and their characteristics for each atom in a system. In Table 3 the latter are collected for the Si_n studied here. This is probably more informative than the averaged mean values.

We see that the differences between individual atoms increase with the size of the clusters and are sensitive for shape. Similar effects in other structures may be of importance insofar as the effective polarizability plays a role in (e.g., chemical, spectroscopic) activity.

B. Model Systems: From Micro- to Macroscopic. All compounds discussed above have no "internal" atoms. For that

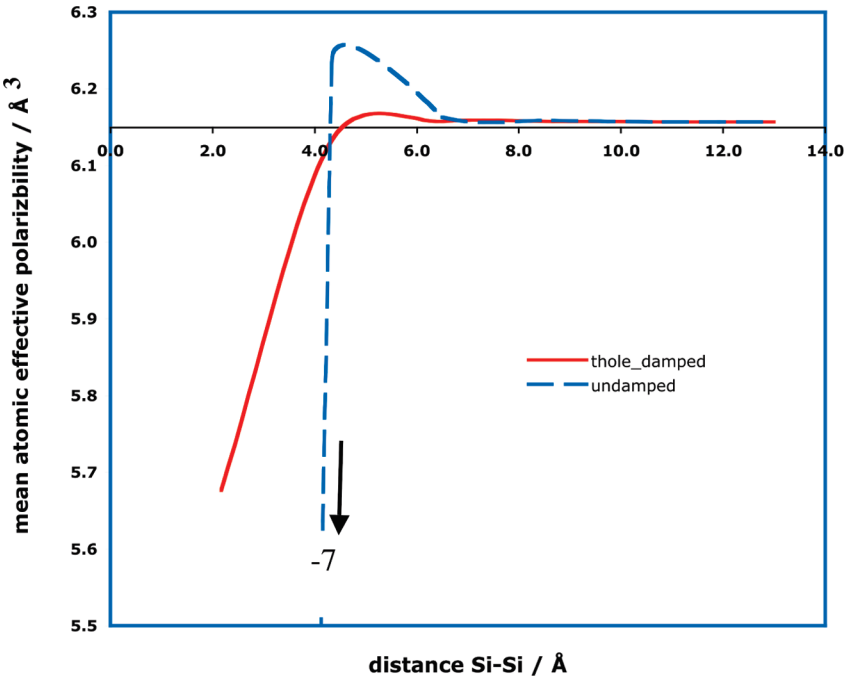

Figure 4. Damped and undamped behavior of $\alpha_{||}$ (cf. eqs 7−12) in Si_2 as a function of the interatomic distance.

TABLE 3: Effective Atomic Polarizabilities from the DRF Calculations (Å^3)

	$\langle\alpha\rangle_{eff}$										
atom Si_n(symm)	1	2	3	4	5	6	7	8	9	10	Δ^a
Si_3 (C_{2v})	5.27	5.42	5.42								0.03
Si_4 (D_{2h})	5.34	5.34	5.02	5.02							0.06
Si_5 (D_{3h})	4.96	4.82	4.82	4.96	4.96						0.03
Si_6 (D_{4h})	4.80	4.80	4.80	4.80	4.63	4.63					0.03
Si_7 (D_{5h})	4.65	4.52	4.65	4.65	4.65	4.65	4.52				0.03
Si_8 (C_{2h})	4.59	4.58	4.58	4.49	4.41	4.41	5.00				0.12
Si_9 (C_{2v})	4.69	4.50	4.34	4.34	4.26	4.26	4.79	4.79			0.11
Si_{10} (C_{3v})	4.69	4.14	4.14	4.14	4.47	4.47	4.47	4.29	4.29	4.29	0.12

^{a} $\Delta = (\langle\alpha\rangle_{max} - \langle\alpha\rangle_{min})/\langle\alpha\rangle_{max}$.

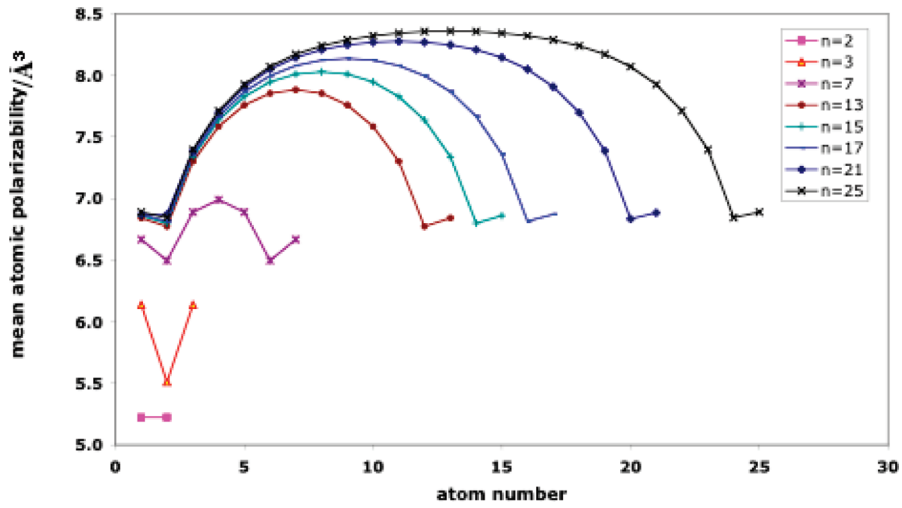

Figure 5. Mean atomic polarizabilities of Si atoms at equal distances of 2.35 Å in some linear model systems, showing saturation for growing chains.

reason we constructed a set of model systems existing of a collection of "Si" atoms. We tried to study what happens when the systems grow. The first model consists of a number of atoms on a line at the same experimental interatomic distance as found in solid silicon (2.351 Å), and further characterized only by the input polarizability, $\alpha_{Si} = 6.16$ Å^3. From them we constructed systems of various size and shape.

In Figure 5 we plotted $\langle\alpha\rangle$ for the individual atoms. In the linear structure the mean atomic polarizability will be larger than the free atom value. This is a result of the head-to-tail coupling of induced dipoles along the bond axis (cf. eq 7). In the linear chains $n = 7-25$ they appear to increase with chain length. However, this sequence shows saturation effects on either end of the chains and on the central atom, which is due to the finite reach of the dipole field as contribution to the local fields. Extension of the chain will only lead to a repetition: more and more atoms will have the same $\langle\alpha\rangle \approx 8$, while the pattern near either end will be the same as in Figure 5: an example of "local anisotropy". In this case, the reach—roughly depending on $\alpha_1\alpha_2/r_{12}^3$—is about seven unit steps but is in general for three-dimensional structures difficult to estimate. If, in the condensed phases, a set of atoms lies on a row parallel with the field, they undergo the head-to-tail increasing effect, but they are also subject to the fields of the induced dipole on adjacent rows that point into the opposite direction. The result is that in general the mean effective polarizabilties in the condensed phases are smaller than those of the constituting monomers.[10,32]

Next, we constructed a number of models of silicon having its diamond structure, starting with a single atom with its nearest neighbor (Si_5), then its next-nearest neighbors (Si_{17}), Si_{191} with a radius of about 10 Å, Si_{1750} with a radius of about 20 Å, and, finally, Si_{4955} with the maximal number of individual polarizabilities for which we could accommodate the relay matrix $\overleftrightarrow{A}$ of eq 5.

In Figure 6 we have plotted $\langle\alpha\rangle$ for each atom—computed with the same parameters as before—as a function of the distance to the central atom. Hence, similar $\langle\alpha\rangle$ values at the same distance coincide in the plot, as is manifest for, e.g., Si_5 and Si_{17}. Pertinent data on these systems are collected in Table 4.

First we point at the difference for Si_5 (D_{3h}) in the preceding section and Si_5 (T_d) in Figure 6: the former has an atomic value $\langle\alpha\rangle_5$ (D_{3h}) = 4.90 Å^3 while the latter has $\langle\alpha\rangle_5$ (T_d) = 5.51 Å^3. Applying an interatomic distance of 2.20 Å in Si_5 (T_d) gives $\langle\alpha\rangle_5$ (T_d) = 5.37 Å^3, demonstrating the importance of the shape of the isomers, the difference being that the D_{3h} molecule has no central atom, in contrast with the T_d case.

The smaller systems show erratic patterns caused by the ragged form of the peripheries: they have been chosen on the basis of distance to the central atom, and therefore they do not necessary lie on completely filled spheres. However, they all show a steep increase at the most distant atoms. For $n = 1750$ the saturation effects are manifest in the plot: all atoms within about 10 Å have almost the same $\langle\alpha\rangle \approx 3.6$ Å^3. In the next 5 Å the average value rises slowly while also the spreading increases, and the last 5 Å shows wildly varying values.

As in the linear systems of Figure 5, the extension of the system results in shifting the graph: for the Si_{4950} system the region with a reasonably converged value is extended by about

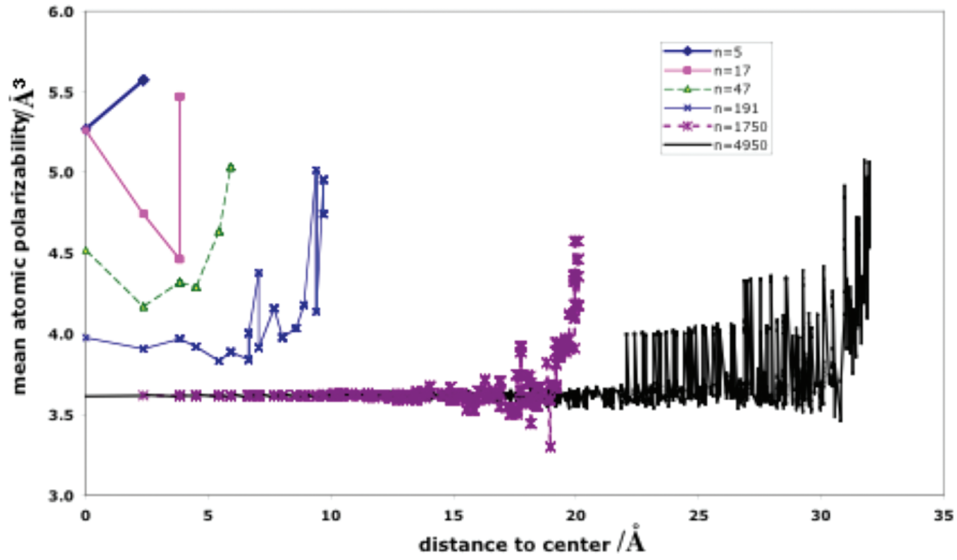

Figure 6. Growing silicon crystal. Mean atomic polarizabilities for each point.

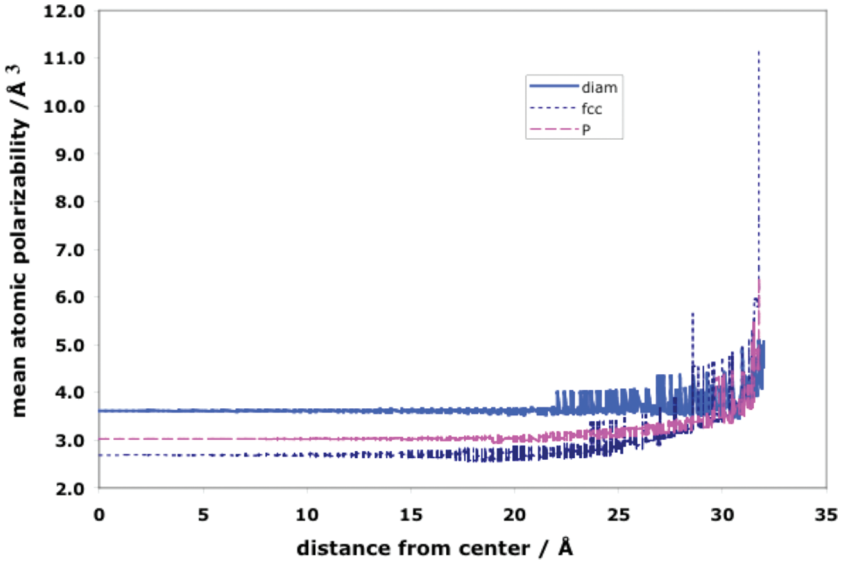

Figure 7. Mean atomic polarizabilities for each point of about 4950 Si atoms in various crystal structures.

TABLE 4: Some Statistical Data for Various "Growing" Crystals

structure	no. of atoms	max	min	average	std dev
diamond	5	5.57	5.27	5.51	0.14
	17	5.47	4.46	5.05	0.45
	47	5.03	4.17	4.53	0.33
	191	5.02	3.83	4.12	0.33
	1750	5.17	3.30	3.71	0.22
	4950	5.08	3.46	3.71	0.18
P	7	7.90	3.92	5.22	1.88
	19	4.32	4.56	4.32	0.32
	4913	6.68	2.96	3.22	0.26
FCC	13	4.61	3.10	3.96	0.60
	19	4.64	3.44	3.84	0.56
	1555	6.36	1.53	2.39	0.57
	4913	11.14	2.57	2.97	0.53

12 Å, at which point again an—even more oscillating—area of about 10 Å ends the plot.

According to Table 4, the Si_{1750} and Si_{4950} systems show an $\langle\alpha\rangle_n = 3.7 \pm 0.2$ Å^3. This implies that we—with a very simple approach and with a minimal number of parameters—"predicted" the dielectric constant of silicon in its experimental structure. Since the atomic volume $\Omega = 19.9$ Å^3 comes straight from the experimental structure used here, the value of $\langle\alpha\rangle_{4950}$ can be used in eq 17 to calculate $\varepsilon \approx 11.5$.

This does not mean that this largest system is a real dielectric: putting unit charges on the central atom and on atom 1755 (at 20.09 Å from the center), we calculate an electrostatic interaction energy of 0.026 hartree and an induction energy of 0.201 hartree. In a dielectric medium the latter should be $0.026(1/12 - 1) = -0.023$ hartree, i.e., an order of magnitude smaller. This seems to confirm Jackson's "rule of thumb"[22] mentioned above. The charges are too close, as is the periphery.

It is also useful to look at the results for systems with other structures: e.g., model crystals with primitive (P) and closed packed (FCC) structures.

In Table 4 we have collected the statistical data for such systems, again for various sizes. Here we see also systems with $\langle\alpha\rangle_n$ smaller than 3.7 Å^3, which have also been found experi-

mentally, albeit smaller than the ones presented here.[1] The difference with the diamond structures is the packing: a diamond structure of hard spheres fills about half the space compared with the FCC structure, while the primitive structure is in between. The smaller atomic volumes in FCC ($\Omega \approx 10$ Å^3) and P ($\Omega \approx 12$ Å^3) lead to stronger (counteracting) local fields and hence lead to smaller $\langle\alpha\rangle_n$.

Jackson et al.[2,5,7] report similar differences in isomers of Si_{19}, Si_{20} and Si_{26} where they distinguish "prolate" and "compact" forms. The compact isomers show smaller computed $\langle\alpha\rangle_n$ than the prolate forms. In Figure 7 the individual atomic results for the $n \approx 4950$ systems are compared.

Although it is on its own satisfying that we can predict the dielectric constant of silicon, there are more important and probably more interesting conclusions to be drawn from Figures 6 and 7.

First, extension of the systems results in "stretching" of the pattern in the plots: the range of saturation will become longer, while the peripherial variations just move outward, while probably preserving their width. In conclusion: a dielectric is at least so large that any local difference from $\langle\alpha\rangle_n$ vanishes in the average, while the always existing, large differences of the "outer skin" do not affect the statistics.

Second, we note that our Si_{4950} systems, with a diameter of about 60 Å, are genuine nanoparticles of which an outer layer of about 10 Å—containing about 15% of the atoms—has properties completely different from the interior. This may be of importance in the fields of nanoparticles, thin films, phase boundaries, and surfaces.

Here lies probably the key to understanding the peculiar spectroscopic properties of nanoparticles.

Our DRF/QM/MM approach is in principle organized such that, e.g., electronic properties of such systems can be investigated without explicitly taking care of all electrons present. This endeavor is obviously beyond the present paper but will be taken up later.

V. Summary and Conclusion

The apostrophes in the title of this paper are meant to emphasize that in molecules, clusters, and the condensed phase in general, an atomic polarizability is an abstraction, and at best a useful parameter in theories and force fields. Therefore, we started this paper with some formal considerations about the essence of dielectrics and microscopic descriptions.

In the practical parts we report results of classical calculations applying the discrete reaction field (DRF) model, using the DRF90-suite[13,14] for getting more insight into the behavior of small Si_n clusters that have average-per-atom polarizabilities, $\langle\alpha\rangle_n$, larger than the bulk value of 3.7 Å^3. For $n = 4-10$ we calculated both the individual polarizabilities and $\langle\alpha\rangle_n$ values. With a single transferable input parameter ($\alpha_{Si} = 6.16$ Å^3, i.e., about the free-atom value), obtained from fitting it to the computed molecular polarizability of Si_3,[4] we reproduced all $\langle\alpha\rangle_n$ in the series accurately. The present results show that there is no need for additional parameters, e.g., for "charge transfer"[7,8] in the analysis or reconstruction of molecular polarizabilities.

Next, we applied the same procedure on Si_n clusters with $n = 5-4950$, having crystal-like structures. We showed that in small clusters the $\langle\alpha\rangle_n$ vary strongly, depend on the shape, and are larger than in the bulk. Starting from $n \approx 1700$ the value of $\langle\alpha\rangle$ of the interior atoms converge while there is always an outer shell of about 10 Å with significantly larger $\langle\alpha\rangle$ that has no statistical influence in the larger systems ($n = 1755$ and 4555). For these systems, with a diamond structure, we arrive at $\langle\alpha\rangle_n = 3.7 \pm 0.2$ Å^3, i.e., the experimental value.

Hence, we have—indirectly—calculated the dielectric constant for silicon, practically from first principles.

Other lattices, primitive and fcc, with tighter packing ratios than the diamond structure, have values smaller than 3.7 Å^3.

All effects on $\langle\alpha\rangle_n$ due to the size and shape of all systems discussed here, can easily be understood in terms of the—properly damped—local fields, which are explicitly and correctly accounted for in our theoretical and practical approach.

We suggest that the different character of the "skin" of nanoparticles, with its different behavior, may be the key to understanding the peculiar properties of these particles.

Acknowledgment. We gratefully acknowledge the constructive comments of a reviewer. P.T.v.D. thanks Dr. R. Havenith (RuG) for useful discussions. The following organizations are thanked for financial support: the Ministerio de Ciencia e Innovación (MICINN, project number CTQ2008-06532/BQU) and the DIUE of the Generalitat de Catalunya (project number 2009SGR528).

Note Added after ASAP Publication. This article was published ASAP on October 20, 2010. Equation 11 and text related to equation 4 have been modified. The correct version was published on October 25, 2010.

References and Notes

(1) Schafer, R.; Schlecht, S.; Woenckhaus, J.; Becker, J. A. *Phys. Rev. Lett.* **1996**, *76*, 471.
(2) Jackson, K.; M., Pederson; Wang, C.-Z.; Ho, K.-M. *Phys. Rev. A* **1999**, *59*, 3685.
(3) Maroulis, G.; Begue, D.; Pouchan, C. *J. Chem. Phys.* **2003**, 119.
(4) Pouchan, C.; Begue, D.; Zhang, D. Y. *J. Chem. Phys.* **2004**, *121*, 4628.
(5) Jackson, K. A.; Yang, M.; Chaudhuri, I.; Frauenheim, Th. *Phys. Rev. A* **2005**, *71*, 033205.
(6) Deng, K.; Yang, J.; Chan, C. T. *Phys. Rev. A* **2006**, *61*, 025201.
(7) Jackson, K.; Yang, M.; Jellinek, J. *J. Phys. Chem. C* **2007**, *111*, 17952.
(8) Guillaume, M.; Champagne, B.; Bégué, D.; Pouchan, C. *J. Chem. Phys.* **2009**, *130*, 134715.
(9) Böttcher, C. J. F.; Bordewijk, P. *Theory of electric polarization*, 2nd ed.; Elsevier: Amsterdam, 1978; Vol. II.
(10) van Duijnen, P. Th.; de Vries, A. H.; Swart, M.; Grozema, F. C. *J. Chem. Phys.* **2002**, *117*, 8442.
(11) Jensen, L.; Swart, M.; van Duijnen, P. Th. *J. Chem. Phys.* **2005**, *122*, 034103.
(12) Jensen, L.; van Duijnen, P. Th. The Discrete Solvent Reaction Field model: A Quantum mechanics/Molecular mechanics model for calculating nonlinear optical properties of molecules in the condensed phase. In *Atoms, molecules and clusters in electric fields. Theoretical approaches to the calculation of electric polarizability*; Maroulis, G., Ed.; Imperial College Press: London, 2006; p 1.
(13) Swart, M.; van Duijnen, P. Th. *Mol. Simul.* **2006**, *32*, 471.
(14) van Duijnen, P. Th.; Swart, M.; Jensen, L. The discrete reaction field approach for calculating solvent effects. *In Solvation Effects on Molecules and Biomolecules: Computational Methods and Applications*; Canuto, S., Ed.; Springer: Berlin, 2008; Vol. 6, p 39.
(15) Silberstein, L. *Philos. Mag.* **1917**, *33*, 521.
(16) Thole, B. T. *Chem. Phys.* **1981**, *59*, 341.
(17) Jensen, L.; Swart, M.; van Duijnen, P. Th.; Snijders, J. G. *J. Chem. Phys.* **2002**, *117*, 3316.
(18) van Duijnen, P. Th.; Swart, M. *J. Phys. Chem. A.* **1998**, *102*, 2399.
(19) Swart, M.; van Duijnen, P. Th.; Snijders, J. G. *J. Mol. Struct. (THEOCHEM)* **1999**, *458*, 11.
(20) Born, M. *Z. Phys.* **1920**, *1*, 45.
(21) van Duijnen, P. Th.; de Vries, A. H. *Int. J. Quantum Chem., Quantum Chem. Symp.* **1995**, *29*, 523.
(22) Jackson, J. D. *Classical Electrodynamics*; John Wiley & Sons: New York, 1975.

(23) Fraga, S.; Saxena, K. M. S.; Karwowski, J. *Handbook of Atomic Data*; Elsevier: Amsterdam, 1976.
(24) Mulliken, R. S. *J. Chem. Phys.* **1955**, *23*, 1833.
(25) Mulliken, R. S. *J. Chem. Phys.* **1955**, *23*, 1841.
(26) Böttcher, C. J. F. *Theory of Electronic Polarisation*; Elsevier: Amsterdam, 1973.
(27) Pouchan, C.; Begue; D. Zhang, D. Y. E-JCPSA6-121-311429; AIP, 2004.
(28) Thole, B. T.; van Duijnen, P. Th. *Theor. Chim. Acta* **1983**, *63*, 209.
(29) Swart, M.; van Duijnen, P. Th.; Snijders, J. G. *J. Comput. Chem.* **2001**, *22*, 79.
(30) van Duijnen, P. Th.; Rullmann, J. A. C. *Int. J. Quantum Chem.* **1990**, *38*, 181.
(31) Fournier, R.; Sinnott, S. B.; DePristo, A. E. *J. Chem. Phys.* **1992**, *97*, 4150.
(32) Jensen, L.; van Duijnen, P. Th.; Snijders, J. G. *J. Chem. Phys.* **2003**, *119*, 12998.

JP1049765